RSC Advances

ROYAL SOCIETY OF CHEMISTRY

www.rsc.org/advances

Journal Name

RSCPublishing

ARTICLE

Enhanced Catalytic Properties of Rhodium Nanoparticles Deposited on Chemically Modified SiO_2 for Selective Hydrogenation of Nitrile Butadiene Rubber

Peng Cao[a], Yanqiang Ni[a], Rui Zou[a], Liqun Zhang[a,b], Dongmei Yue[a,b]*

Cite this: DOI: 10.1039/xoxxoooooox

Received ooth January 2012,
Accepted ooth January 2012

DOI: 10.1039/xoxxoooooox

www.rsc.org/

An efficient and recyclable catalyst was prepared by depositing rhodium nanoparticles (Rh NPs) on a SiO_2 support with surface modified by 3-aminopropyl-trimethoxysilane (APTS). The obtained catalyst, Rh(Ⅲ)/$MSiO_2$, was extensively characterized by FTIR, SEM, XRD, XPS, BET, and ICP to demonstrate the incorporation of amine groups on the surface of modified SiO_2. The hydrogenation of acrylonitrile butadiene rubber (NBR) was used to evaluate the catalytic properties of Rh(Ⅲ)/$MSiO_2$, and a 98.68% conversion and nearly 100% selectivity to C=C were obtained under optimum condition (120 ℃, 3.0 MPa H_2, 8 h). A comparative study was made between Rh(Ⅲ)/$MSiO_2$ and Rh(Ⅲ)/SiO_2 in the hydrogenation of NBR, and Rh(Ⅲ)/$MSiO_2$ showed higher activity and higher stability. The results indicated that the increase of amount of deposited metal particles and improvement of the adhesion of metal particles to the support are the reasons for high performance of Rh(III)/$MSiO_2$. In addition, the Rh(Ⅲ)/$MSiO_2$ could be easily recovered by centrifugation and reused for 3 times with a few loss in activity and selectivity. Furthermore, this modified method can be extended to other heterogeneous catalyst systems to improve their activity, recyclability and stability.

1. Introduction

The catalytic hydrogenation of unsaturated polymers is one of the effective methods to prepare products that exhibit improved mechanical, chemical, and thermal properties over those of the original polymers.[1-5] The hydrogenation of acrylonitrile butadiene rubber (NBR) is a representative example to produce hydrogenated acrylonitrile butadiene rubber (HNBR), a polymer that shows excellent resistance to thermal and oxidative degradation. Due to the increasing demand of HNBR on the market of high performance elastomers, the hydrogenation of NBR has attracted significant attention.

Generally, the hydrogenation of NBR can be realized by heterogeneous or homogeneous processes depending on the nature of the catalyst.[6, 7] Homogeneous hydrogenation allows the reaction to be carried out at milder operating conditions and without diffusion problems.[6, 8-11] Nevertheless, the removal of expensive catalysts from the final polymer product, i.e., HNBR, is often difficult, and the residual catalysts in the product can cause polymer degradation. Therefore, in order to decrease the production cost, the heterogeneous systems have received much attention as an alternative to the use of conventional homogeneous catalysts in the past few decades and has been applied to the hydrogenation of diene-based polymers. The heterogeneous systems can be defined as modified homogeneous catalysts to "break" the uniformity of the catalyst and products by making them in separate phases to allow their separation.[12] The simplest method is to immobilize homogeneous catalysts on various types of organic and inorganic supports.[13] The most widely explored heterogeneous catalysts for hydrogenation of NBR are Pd/C, Pd/SiO_2, and Pd/TiO_2, all of which have been developed by Zeon Corporation since the 1980s. With these catalysts, a degree of hydrogenation of above 95% can be achieved.[14, 15] However, the Pd nanoparticles have poor adhesion to the bare support due to the absence of chemical bonding, which will lead to the leaching of active Pd particles from the support surface during the reaction. The catalyst Pd/SiO_2 was found to give decreasing degree of hydrogenation from 98.8% to 33.3% after one times recycling.[15] Also, the high viscosity of the polymer solution and the steric hindrance of the polymer chains lead to limited contact between the polymer and the supported catalysts. Further, in recent years, little effort has been directed towards the development of new heterogeneous catalytic systems for hydrogenation of NBR with good activity and recyclability.[6] Therefore, researches in this area are urgently needed to optimize the heterogeneous NBR hydrogenation process.

The amount and quality of deposited active metal particles depend on the surface properties of the support.[16, 17] Because of the absence of chemical bonding, the metal particles usually display poor adhesion to the support, resulting in their easy removal from the support surface during reactions. Nevertheless, surface modification with organic functional groups has been found to be useful for increasing the amounts of the metal particles loaded and improving the adhesion between the metal particles and the support.[18, 19] In previous investigations, APTS was one of the most commonly used coupling agents for modifying the SiO_2 surfaces.[20-22] And, modified SiO_2 plays a vital role in the development of materials for various applications, such as adsorption of metal ions, catalysis and drug delivery.[23-26] In addition, this method overcomes the problems of metal leaching in comparison with the ion exchange or adsorption methods used for immobilization on porous supports.[20] Therefore, in this study, APTS was chosen as a modifier to enhance the metal loading and improve the properties of the supported catalysts.

To the best of our knowledge, Rh NPs loaded on surface-modified SiO_2 have not been studied for the hydrogenation of NBR. Herein, the purpose of this research was to fabricate a surface modified SiO_2 immobilized Rh NPs catalyst, which acts as a highly active, selective and easily recyclable catalyst for hydrogenation of NBR. Also, a comparative study of the Rh(Ⅲ)/$MSiO_2$ and Rh(Ⅲ)/SiO_2 was also performed. The catalytic activity, selectivity, and recyclability were evaluated to better understand the importance of modification.

2. Experimental

2.1 Materials SiO_2 with different particle sizes (40 nm, 1 μm, 10 μm, 48 μm, and 150 μm) was purchased from XF NANO, Inc. The rhodium precursor $RhCl_3{\cdot}3H_2O$ was purchased from Shanghai Jiulin Chemical Co., Ltd., with an Rh content of 39.0 wt%. Nitrile rubber (Nancar1052M30) was obtained from Taiwan NANTEX Chemical Industry Co., Ltd., with a number average and a weight average molecular weight of 108 and 307 kg/mol, respectively, as measured by gel permeation chromatography with tetrahydrofuran (THF) as the solvent at 35 ℃. 3-aminopropyl-triethoxysilane (APTS) was purchased from Tianjin Guangfu Research Institute of Fine Chemicals. Chlorobenzene (AR), anhydrous ethanol (AR), acetone (AR), and ammonia (25 wt%) were all obtained from Beijing Chemical Factory. Triphenylphosphine and deuterated chloroform were obtained from National Chemical Reagent Co., Ltd. Nitrogen (research grade; N_2＞ 99.99%) and hydrogen (research grade; H_2＞99.99%) were donated by Beijing Beifen Gas Industries Co., Ltd.

2.2 Preparation of Modified Silica ($MSiO_2$) The SiO_2 was modified with APTS in order to covalently attach a -NH_2 termination to its surface according to published procedures.[27] SiO_2 (5.0 g, dried under vacuum at 100 ℃ for 6 h before use) was first dispersed into 200 mL of deionized water under stirring at room temperature for 15 min to form slurry. APTS (2 mL) was added into the slurry slowly, and heated to 40 ℃ for 1 h. Then, 8 mL of ammonia (25 wt%) was added dropwise to promote the reaction, and the slurry was further stirred at 40 ℃ for another 2 h. After reaction, the mixture was sonicated for 15 min, recovered by filtration, and washed with copious amounts of fresh deionized water in order to remove the loosely bound APTS. Finally, the $MSiO_2$ was dried at 80 ℃ overnight.

2.3 Preparation of Supported Catalysts The $MSiO_2$ (2.5 g) was impregnated in 50 mL of deionized water and dispersed for 30 min in an ultrasonic bath. 5 mL of $RhCl_3{\cdot}3H_2O$ solution (10 g/L) was added to the suspension, following by stirring vigorously for 10 h. Because the amine group is a strong electron donor having a strong capability for chelating to transition metal ions, Rh^{3+} can react with -NH_2 to form a complex and be bound to the SiO_2 surface. After impregnation, the slightly yellow powder was recovered by filtration, washed with deionized water for several times, and dried under vacuum at 80 ℃ for 12 h. The powder sample was designated as Rh(Ⅲ)/$MSiO_2$ **1**. The Rh(Ⅲ)/$MSiO_2$ **1** was later reduced by $NaBH_4$ as follows: Rh(Ⅲ)/$MSiO_2$ **1** (2.5 g) was dispersed into deionized water (200 mL) under stirring for 30 min. Then, a freshly prepared $NaBH_4$ solution (1.0 g of $NaBH_4$ in 30 mL of deionized water) was added dropwise into the mixture, stirring for an additional 3 h. The final solids were recovered by filtration, washed repeatedly with deionized water, dried under vacuum, and stored in a glass bottle for further use. The sample was designated as Rh(0)/$MSiO_2$ **2**. The preparation processes of Rh(Ⅲ)/$MSiO_2$ **1** and Rh(0)/$MSiO_2$ **2** are illustrated in Scheme **1**.

For comparison, under the same conditions, the SiO_2 without modification was impregnated with an aqueous solution of $RhCl_3{\cdot}3H_2O$ to form Rh(Ⅲ)/SiO_2 **3**, which was then reduced with $NaBH_4$ to form Rh(0)/SiO_2 **4**. The surface features of Rh(Ⅲ)/SiO_2 **3** and Rh(Ⅲ)/$MSiO_2$ **1** are shown in the Fig. **S1**.

2.4 Catalytic Activity for Hydrogenation of NBR The hydrogenation reaction was carried out in a 500-mL high pressure reactor. The NBR chlorobenzene solution (3 wt%) and catalyst were placed into the reactor. Before being heated to the reaction temperature, the reactor was degassed with N_2 for 3 times to remove air. Then the reactor was heated to the desired temperature, and the reaction was initiated by flushing H_2 to 3.0 MPa and adjusted the agitation rate to 480 rpm. The hydrogen pressure and reaction temperature were kept constant throughout the reaction. The conversion of the double bonds, also called the degree of hydrogenation (HD), was calculated as:

$$HD = (1 - [C=C]_t / [C=C]_0) \times 100\% \quad (1)$$

where $[C=C]_t$ is the concentration of C=C bonds at reaction time t and $[C=C]_0$ is the initial double bond concentration. The hydrogenated NBR sample was analyzed by ^{1}HNMR.[28]

2.5 Catalyst Recovery After each hydrogenation reaction, catalyst was removed from the NBR glue by centrifugation (8000rpm/min for 30 min). Then the catalyst washed with acetone for 3-4 times followed by decantation and dried under vacuum at 60 ℃ for subsequent reaction.

2.6 Catalyst Reactivation A known amount of recovered catalyst and 100 mL of chlorobenzene were transferred into a flask, heated to 60 ℃ in an oil bath, stirring vigorously for 8 h. Then, the catalyst was separated from the chlorobenzene and dispersed in acetone overnight in an Erlenmeyer flask. The final recovered catalyst was obtained by centrifugation, fully washed with acetone and ethanol, and dried under vacuum at 60 ℃ for use in the next hydrogenation reaction.

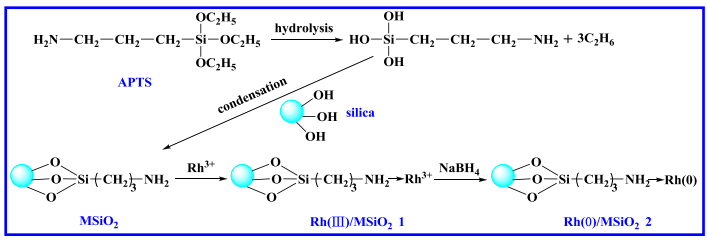

Scheme 1. Preparation of supported catalysts.

2.7 Characterization The physical and chemical properties of the prepared samples were measured by several methods. FTIR spectra were obtained by a Bruker Tensor 27 spectrophotometer in the wave-number range of 400-4000 cm^{-1}. The morphology and particle size of the samples were examined by scanning electron microscopy (SEM, Hitachi S4800 Dual Stage Electron Microscope) at 10 kV. The crystal phases of the samples were determined by X-ray diffraction (XRD, Bruker D8 Advance) at a scanning rate of 0.02 °/s in the 2θ range of 5 °to 90 °. The specific surface area, pore size distribution, pore volume, and adsorption-desorption isotherms of the samples were measured by N_2 physical adsorption at 77 K (Micrometrics ASAP-2020M adsorption apparatus). X-ray photoelectron spectroscopy (XPS) was performed on a Thermo Fisher Scientific ESCALAB 250 system with monochromatized Al KR radiation at 15 kV. A thin layer of the sample was dispersed on the surface of a carbon tape, evacuated in a load lock, and then transferred into the analysis chamber for measurement. The Rh concentration in the samples was determined by using Inductive Coupled Plasma (ICP) Optical Emission Spectroscopy (ICPS-7500). For ICP analyses, the samples were digested in 10% (v/v) nitric acid and 40 wt% hydrogen fluoride (HF) at 120 ℃ for 30 min.

3. Results and Discussion

3.1 Characterization of Supported Catalysts

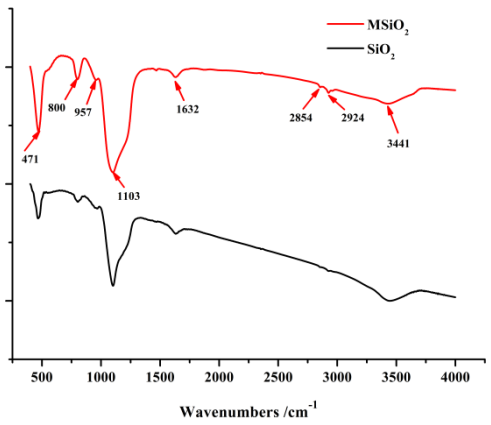

Fig. 1. FTIR spectra of SiO_2 and $MSiO_2$.

The changes in chemical structure of SiO_2 modified with APTS were investigated by FTIR, as shown in Fig. **1**. The intensities of the peaks of APTS are weak due to the low concentration. The peak at 471 cm^{-1} attributed to the bending vibration of Si-O-Si; the peaks at 800 cm^{-1} and 1103 cm^{-1} represent the asymmetric and symmetric stretching vibrations of Si-O; and the peaks at 1103 cm^{-1} and 3441 cm^{-1} are the characteristic peaks of the hydroxyl groups on the SiO_2 surface. For $MSiO_2$, however, in addition to the absorption peaks in SiO_2, the peak at 3441 cm^{-1} broadens, having a clear shoulder structure around 3378 cm^{-1}, which is the characteristic peak of N-H stretching vibration, and the peaks for the bending vibrations of the $-CH_2$ and $-CH_3$ structures at 2924 cm^{-1} and 2854 cm^{-1} become more visible, but the band at around 1632 cm^{-1} appears slightly less intense, indicating successful incorporation of APTS onto the SiO_2.

Fig. **S2** shows that the interface of SiO_2 particles is indistinct, whereas the $MSiO_2$ particles remain relatively well dispersed. The large numbers of hydroxyls on the surface of SiO_2 generate strong hydrogen bonding, resulting in aggregation of SiO_2 particles. After modification, the APTS reacts with the hydroxyls on the surface of SiO_2, leading to a decreased hydrogen bonding interaction. In addition, the surface tension of SiO_2 decreases after hydrolysis and condensation, and APTS can act as a physical barrier to prevent the SiO_2 particles from re-aggregation. Therefore, the particles of $MSiO_2$ display a well-dispersion compare with that of SiO_2. Both Rh(Ⅲ)/SiO_2 **3** or Rh(Ⅲ)/$MSiO_2$ **1** consists of small particles of 40-60 nm in diameter, and the latter is slightly better dispersed than the former.

The XRD patterns of $RhCl_3$, SiO_2, $MSiO_2$, Rh(Ⅲ)/SiO_2 **3**, and Rh(Ⅲ)/$MSiO_2$ **1** are illustrated in Fig. **2**. It can be seen that $RhCl_3$, SiO_2, $MSiO_2$, Rh(Ⅲ)/SiO_2 **3** and Rh(Ⅲ)/$MSiO_2$ **1** all present the characteristic peak of amorphous SiO_2 at 24.40 °, indicating the structure of SiO_2 is well preserved after modification. However, the peaks at 15.51 °, 36.75 °, 52.75 °, and 65.94 °, corresponding to the (001), (131), (060), and (004) planes, respectively, of Rh, are not observed in Rh(Ⅲ)/SiO_2 **3** and Rh(Ⅲ)/$MSiO_2$ **1** because of (1) the strong diffraction

peak of SiO_2 hiding the weak diffraction peak of Rh element; (2) the small amount of Rh, which is difficult to detect; (3) the poor dispersion of Rh ion on the surface of SiO_2; and (4) the Rh ion infiltrating into the pores of SiO_2.

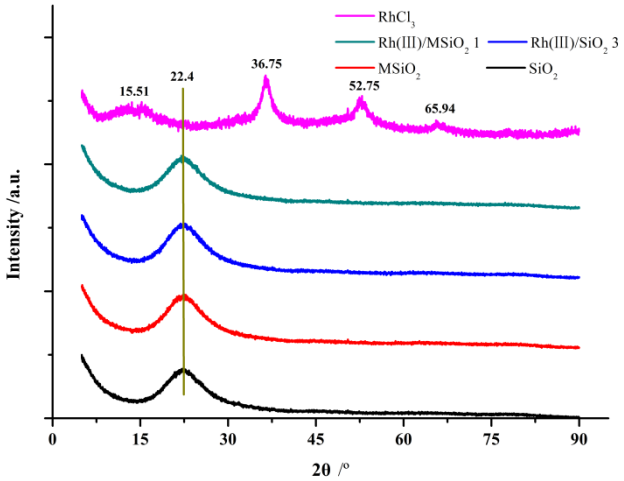

Fig. 2. XRD-patterns of $RhCl_3$, SiO_2, $MSiO_2$, Rh(Ⅲ)/SiO_2 **3** and Rh(Ⅲ)/$MSiO_2$ **1**.

N_2 adsorption/desorption isotherms were used to determine the changes in the BET surface area, pore volume, and average pore diameter of SiO_2 and $MSiO_2$, and the results were shown in Fig. **S3**. The calculated surface area, pore volume, and pore diameter are listed in Table **S1**. This information is useful for comparing the adsorption properties of SiO_2 and $MSiO_2$. The obtained isotherms for the SiO_2 and $MSiO_2$ show reversible type IV behavior.[29] After modification, the pores of SiO_2 are filled with APTS, leading to a decrease in average pore diameter. Therefore, the surface area and pore volume of $MSiO_2$ are smaller than those of SiO_2, indicating successful modification by APTS.

XPS survey was conducted to study the attachment of APTS layer onto the SiO_2. The XPS spectra of SiO_2 and $MSiO_2$ are shown in Fig. **S4**. The main components of SiO_2, such as O and Si, exhibit strong absorption intensity. An absorption peak with low intensity near 400 eV is detected for the $MSiO_2$ due to the nitrogen atom from APTS. There is a distinct increase in the absorption intensity of the C 1s peak because the propyl chains of APTS are adsorbed onto SiO_2. In the case of SiO_2, the C 1s peak is mainly due to adventitious carbon contamination.

The XPS Si 2p and N 1s spectra of SiO_2 (a, c) and $MSiO_2$ (b, d), respectively, are seen in Fig. **3**. In the Si 2p spectrum of SiO_2, the peak at BE ~103.72 eV is characteristic of the Si^{4+} in SiO_2; a smaller peak at BE ~105.92 eV indicates the presence of Si-OH species. For the $MSiO_2$, the characteristic peak of Si^{4+} is at a BE of ~103.72 eV and the Si-OH peak is at 105.69 eV. The important data from the XPS Si 2p spectra are calculated in Table **S2** and Table **S3**. The ratio of the Si^{4+} to Si-OH is approximately 97.66/2.34 for SiO_2, but nearly 100/0 for $MSiO_2$. The reason for the disappearance of the Si-OH peak in $MSiO_2$ is the formation of Si-O-Si bonds during the modification process.

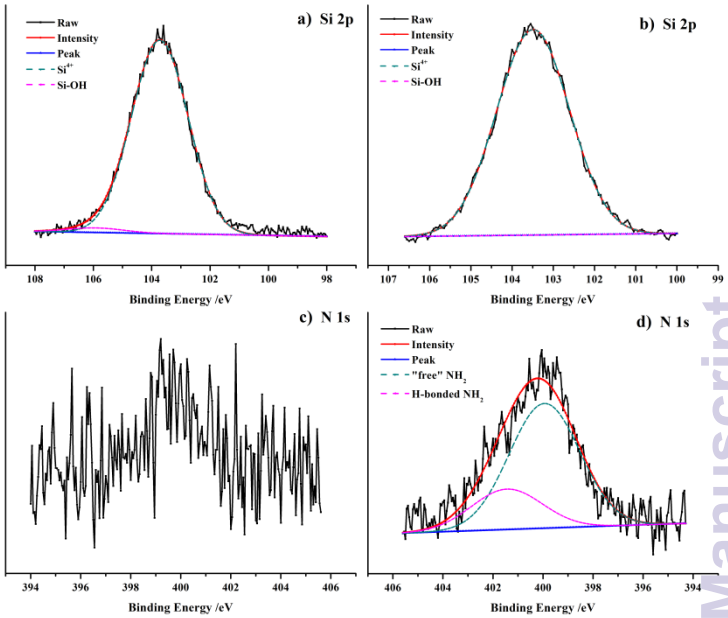

Fig. 3. X-ray photoelectron spectra of (a, c) SiO_2 and (b, d) $MSiO_2$.

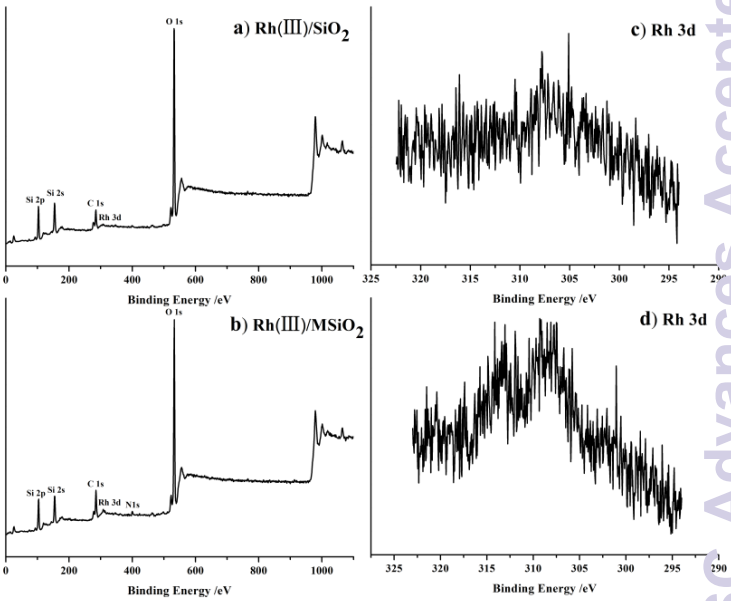

Fig. 4. XPS survey spectra (a) Rh(Ⅲ)/SiO_2 **3** and (b) Rh(Ⅲ)/$MSiO_2$ **1**; XPS Rh 3d spectra for (c) Rh(Ⅲ)/SiO_2 **3** and (d) Rh(Ⅲ)/$MSiO_2$ **1.**

The presence of APTS on the surface of SiO_2 was further confirmed by the N 1s spectrum of $MSiO_2$ in Fig. **3d.** It shows two peaks attributable to the hydrogen-bonded NH_2 of APTS at about 401.3 eV and the "free" NH_2 terminal groups of APTS, which are not hydrogen bonded, at ~399.8 eV. An extremely weak signal in the N 1s spectrum of the SiO_2 may be due to adventitious nitrogen contamination. The relatively strong peak at a BE of ~400 eV in the N 1s spectrum of $MSiO_2$ indicates that the surface of SiO_2 has been successfully modified. For $MSiO_2$, the ratio of the hydrogen

bonded NH_2 to the "free" NH_2 is approximately 76/24. The important data from the XPS N 1s spectra of $MSiO_2$ are presented in Table **S4**.

Table 1. Surface compositions (in atom**%**) of Rh(Ⅲ)/SiO_2 **3** and Rh(Ⅲ)/$MSiO_2$ **1**

Samples	C (%)	O (%)	Si (%)	N (%)	Rh (%)	C/O (%)
Rh(Ⅲ)/SiO_2 **3**	13.61	55.95	30.06	0.21	0.16	24.33
Rh(Ⅲ)/$MSiO_2$ **1**	18.92	51.03	27.55	1.88	1.22	37.08

The main components of the two catalysts, Rh(Ⅲ)/SiO_2 **3** and Rh(Ⅲ)/$MSiO_2$ **1,** such as Si and O, exhibit strong absorption intensity, while Rh shows relatively weak absorption intensity due to its low concentration (Fig. **4**). Table **1** reports the surface composition (in atom%) of the Rh(Ⅲ)/SiO_2 **3** and Rh(Ⅲ)/$MSiO_2$ **1** samples as determined by XPS. The Rh concentration increases eightfold after modification. The weak peak in the Rh 3d spectrum of Rh(Ⅲ)/SiO_2 **3** is attributed to the low rhodium content of 0.16 atom%, which is too low for detection by XPS. The increase in the C/O atomic ratio from 24.33% in Rh(Ⅲ)/SiO_2 **3** to 37.08% in Rh(Ⅲ)/$MSiO_2$ **1** also confirms that the SiO_2 has been successfully modified by APTS.

3.2 Catalytic performance of rhodium catalysts

The as-prepared rhodium catalysts were used in hydrogenation of NBR to evaluate the catalytic behaviour. Table **2** compares the catalytic performance of the various rhodium catalysts for hydrogenation of NBR under similar conditions.

Table 2. Catalytic performance of various rhodium catalysts for hydrogenation of NBR

Catalysts	$W_{cat.}/W_{NBR}$	W_{PPh3}/W_{NBR}	HD /%[a]
Rh(0)/SiO_2 **4**	0.05	0	＜5
Rh(0)/SiO_2 **4**	0.05	0.025	8.46
Rh(0)/$MSiO_2$ **2**	0.05	0	6.81
Rh(0)/$MSiO_2$ **2**	0.05	0.025	22.57
Rh(Ⅲ)/SiO_2 **3**	0.05	0.025	52.44
Rh(Ⅲ)/$MSiO_2$ **1**	0.05	0.025	98.68

Note: [a]HD =degree of hydrogenation, $W_{cat.}$=weight of rhodium catalyst, W_{NBR}=weight of NBR, and W_{PPh3}=weight of triphenylphosphine. The reaction is conducted at 3.0 MPa of pressure of H_2 and 120 ℃ for 8 h.

It can be seen that the degree of hydrogenation is very low for Rh(0)/SiO_2 **4** and Rh(0)/$MSiO_2$ **2**. A possible reason is that Rh^0 has low activity towards NBR. However, under identical reaction conditions, the degree of hydrogenation increases to 8.46% and 22.57%, respectively, for Rh(0)/SiO_2 **4** and Rh(0)/$MSiO_2$ **2** with triphenylphosphine (PPh_3) as assistant agent. The reason can be attributed to the chemical adsorption of PPh_3 on the surface of the catalyst, promoting in situ growth of the active $Rh^{\delta+}$ ($0<\delta\leq1$) species,[30] which is beneficial to the catalytic hydrogenation of NBR. This observation also suggests that the activity of these catalysts is largely associated with the situ growth of the active species $Rh^{\delta+}$ ($0<\delta\leq1$), rather than the Rh^0.

The degree of hydrogenation is 52.44% and 98.68% for Rh(Ⅲ)/SiO_2 **3** and Rh(Ⅲ)/$MSiO_2$ 1, respectively, with PPh_3 as assistant agent. The high degree of hydrogenation is attributed to the in situ growth of the Rh^+ active species between Rh^{3+} and PPh_3.

The degree of hydrogenation was determined by ^{1}HNMR. Fig. **5** shows the ^{1}HNMR spectra of (a) NBR and (b) HNBR. It can be seen that Rh(Ⅲ)/$MSiO_2$ **1** shows higher activity than Rh(Ⅲ)/SiO_2 **3** for hydrogenation of NBR under the same conditions. All the peaks in the olefinic proton region have disappeared in the spectrum for Rh(Ⅲ)/$MSiO_2$ **1**, which gives a degree of hydrogenation of 98.68%, higher than the degree of hydrogenation of 52.44% for Rh(Ⅲ)/SiO_2 **3**, which remained a few olefinic chains. The characteristic peaks for -NH_2 and -NH- are not observed in the ^{1}HNMR spectrum of Rh(Ⅲ)/$MSiO_2$ **1**, indicating that the catalyst is selective in the hydrogenation of NBR, which takes place on the C=C double bonds without reduction of the -CN group.

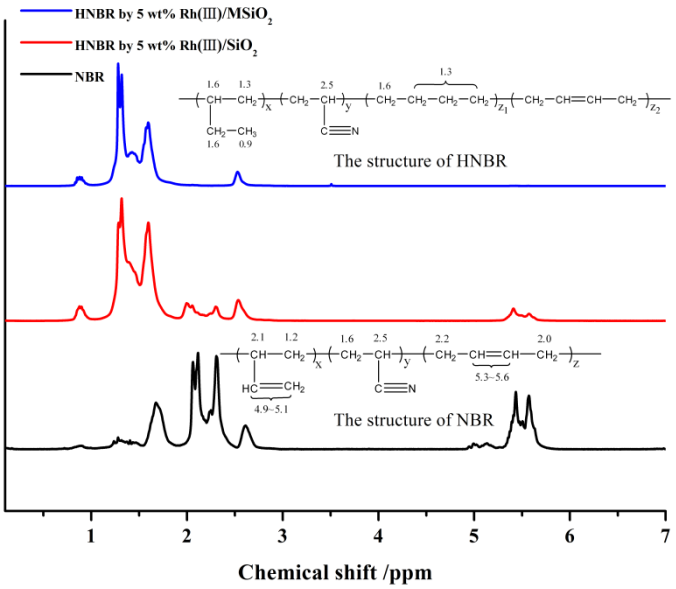

Fig. 5. ^{1}HNMR spectra of (a) NBR and (b) HNBR.

To understand the underlying mechanism that lead to the higher activity of Rh(Ⅲ)/$MSiO_2$ **1** than that of Rh(Ⅲ)/SiO_2 **3** for hydrogenation of NBR, we focus on the cause for the different activity between the two catalysts. In a previous research,[27] the activity of a catalyst was strongly affected by the amount of metal active centers and their dispersion. In this study, because the -NH_2 groups on the surface of $MSiO_2$ can significantly affect the adsorption of metal ions, we hypothesized that the utilization of APTS increases the amount of the rhodium loaded and improves the adhesion

between the rhodium ions and the $MSiO_2$. Comparison experiments were carried out to confirm this hypothesis.

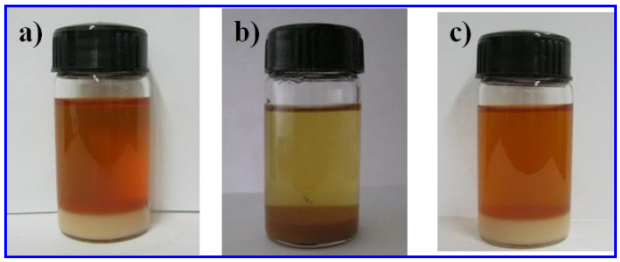

Fig. 6. Images of different silica supports, (a) SiO_2, (b) $MSiO_2$, and (c) $MSiO_2$ calcined, impregnated with $RhCl_3$ solution.

First, the $MSiO_2$ was calcined at 550 ℃ for 4 h to remove the -NH_2 groups on its surface. Then, the calcined $MSiO_2$ was impregnated with $RhCl_3$ solution (see Fig. **6c**) to fabricate the supported catalyst Rh(Ⅲ)/$MSiO_2$ with calcination. The variations of the degree of hydrogenation for different catalysts are shown in Fig. **7**. The catalytic performance of Rh(Ⅲ)/$MSiO_2$ with calcination is similar to that of Rh(Ⅲ)/SiO_2 **3** because of the removal of the -NH_2 by calcination. The results indicates that APTS plays a key role in increasing the amount of rhodium loaded and enhancing the adhesion between the rhodium ions and the $MSiO_2$ support, causing the higher activity of Rh(Ⅲ)/$MSiO_2$ **3** than that of Rh(Ⅲ)/SiO_2 **1**.

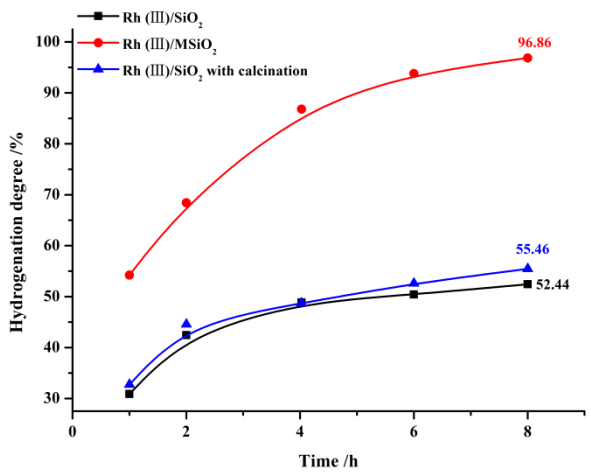

Fig. 7. Degree of hydrogenation as function of time for various silica-supported catalysts: Rh(III)/SiO_2, Rh(III)/$MSiO_2$, and Rh(III)/$MSiO_2$ with calcination. Reaction conditions: NBR solution (200 mL, 3 wt%), rhodium supported catalyst (0.30 g, 5 wt%), and triphenylphosphine (0.15 g, 0.25 wt%) were heated at 120 ℃ under H_2 pressure of 3.0 MPa.

Different solvents, such as water, a mixture of water/ethanol (volume ratio=1:1), and ethanol were investigated to optimize the surface coating process for the modification of SiO_2. The catalytic performance of Rh(Ⅲ)/$MSiO_2$ **1** prepared by using different solvents is illustrated in Table **S5**. All three solvents give a similar degree of hydrogenation, implying that the use of these solvents results in similar amounts and dispersion of surface Rh NPs.

The support has an effect on catalyst selectivity as well as activity.[31, 32] Therefore, we also investigated the hydrogenation of NBR, using catalyst Rh(Ⅲ)/$MSiO_2$ **1** with different SiO_2 particles sizes: 40 nm, 1 μm, 10 μm, 48 μm, and 150 μm. It shows that the degree of hydrogenation increases with decreasing particle size of SiO_2 because of the increase in surface area (see Table **S6**). However, Rh(Ⅲ)/$MSiO_2$ **1** with a particle size of 1 μm exhibits a higher degree of hydrogenation than Rh(Ⅲ)/$MSiO_2$ **1** with a particle size of 0.04 μm because the large NBR coils cannot access the micro- and mesopore structures of the SiO_2, where the active Rh species are located.

Of the catalysts prepared in this study, Rh(Ⅲ)/$MSiO_2$ **1** with a particle size of 48 μm exhibited relatively high activity, selectivity, and separation for the hydrogenation of NBR. In the following investigations, we used only the heterogeneous catalyst system of Rh(Ⅲ)/$MSiO_2$ **1** with a particle size of 48 μm and PPh_3 as ligand for the hydrogenation of NBR.

The effects of various conditions, such as reaction temperature, time, and pressure, concentration of NBR, and concentration of catalyst, on the hydrogenation of NBR using Rh(Ⅲ)/$MSiO_2$ **1** are shown in Fig. **S5**. Each factor was studied in turn, all other factors being kept constant. The degree of hydrogenation gradually increases with increasing reaction time and concentration of catalyst. The degree of hydrogenation increases with increasing temperature, reaches a maximum at about 120 ℃, and then decreases with further increases in temperature, probably because of catalyst deactivation. Similarly, the degree of hydrogenation reaches a maximum of 98.40% at a concentration of NBR of 3 wt%. The degree of hydrogenation decreases with further increases in the concentration of NBR because the increasing viscosity of the NBR solution limits diffusion. The degree of hydrogenation increases with increasing hydrogen pressure because of the limited solubility of H_2 gas in the solvent.

Therefore, we concluded that the modification of SiO_2 can effectively improve the amount of active rhodium species and enhance the adhesion between the rhodium ions and the $MSiO_2$ support. The superior catalytic performance of Rh(Ⅲ)/$MSiO_2$ **1** is ascribed to its superior physicochemical properties.

3.3 Reusability of Rh(Ⅲ)/$MSiO_2$ 1

A significant advantage of heterogeneous catalyst is the ability to easily remove from the reaction mixture and reuse it for subsequent reactions.[33, 34] The reusability of Rh(Ⅲ)/$MSiO_2$ **1** was examined for the hydrogenation of NBR at 120 ℃ under high pressure by using 5 wt% of catalyst with a Rh loading of 1.18 wt%. The results of the recycling experiments are shown in the Table **3**.

Table 3. Hydrogenation of NBR catalyzed by recycle catalyst of Rh(Ⅲ)/$MSiO_2$ **1**

Recycle	1	2	3	4[a]
HD (%)	98.53	90.35	67.61	81.66

Note: 1: the fresh catalyst; 2, 3: the used catalyst; 4a: the reactivated catalyst. Reaction conditions: concentration of NBR solution=3 wt%, concentration of catalyst=5 wt%, $W_{PPh3}/W_{cat.}$= 0.5, P_{H2}=3.0 MPa, and T=120 ℃;

In a previous research,[15] a Pd/SiO_2 catalyst lost about 65% of its activity in the hydrogenation of NBR after one continuous cycles, whereas Rh(Ⅲ)/$MSiO_2$ **1** lost about 8.18% under the same conditions. The results indicate that the catalytic stability of Rh(Ⅲ)/$MSiO_2$ **1** is superior to that of Pd/SiO_2. In the Rh(Ⅲ)/$MSiO_2$ **1** system, the SiO_2 was modified by APTS before the conventional impregnation process, and thus the Rh NPs are attached to the SiO_2 surface with chemical bonds, as shown in Scheme **1**. However, in the Pd/SiO_2 system, the Rh NPs were attached to the SiO_2 surface with van der Waals forces. Because the binding force of a covalent bond is much stronger than the van der Waals forces, it is harder for the Rh NPs to detach from the SiO_2 surface and higher stability can be obtained.

Also, to understand the deactivation mechanism of the Rh(Ⅲ)/$MSiO_2$ **1**, we carried out leaching experiments to determine whether the hydrogenation reaction occurs with the Rh species on the support surface or the leached homogeneous Rh species.

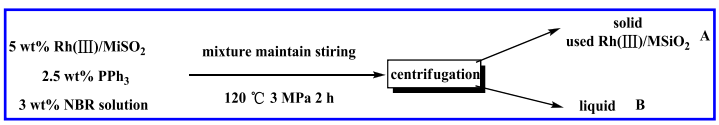

Scheme **2**. Leaching experiment for Rh(Ⅲ)/$MSiO_2$ **1** for hydrogenation of NBR.

Rh(Ⅲ)/$MSiO_2$, PPh_3, and NBR solution were added into a 500-mL high pressure reactor, maintaining stirring at 120 ℃ for 2 h, and the reaction products were centrifuged to obtain a solid catalyst Rh(Ⅲ)/$MSiO_2$ (**A**) and liquid (**B**) (Scheme **2**). Both the solid (**A**) and the liquid (**B**) were used for next hydrogenation reaction; the result is shown in the Fig. **S6**. When the recycled catalyst (**A**) was used for the hydrogenation of NBR, HNBR was obtained with a degree of hydrogenation of 87.32%. In contrast, when the liquid (**B**) was allowed to react under similar conditions, but without a catalyst, the degree of hydrogenation was only 11.86%. The result shows that the leaching of a small amount of Rh species occurred due to the viscous NBR solution, high temperature, and high pressure. Therefore, the leaching of Rh species is one of the reasons giving rise to the decrease in activity. Also, the amount of leaching Rh species in the recovered catalyst can be verified by ICP analysis. Table **S7** shows that after two consecutive cycles, the rhodium amount in the recovered catalyst is 0.98 wt %, which is 83% of the initial rhodium content in the fresh catalyst. Also, it should be noted that the rhodium amount decreases from the first to the second run and then remains constant.

SEM was employed to investigate the evolution of the morphology of the recycled Rh(Ⅲ)/$MSiO_2$ **1** (Fig. **S7**). It can be seen that the Rh NPs re-aggregate and a thin film covers the surface of the SiO_2, possibly because of the high viscosity of the NBR solution, thus resulting in a decrease in activity. In addition, XPS and FITR demonstrate that the chemical structure of reused catalyst Rh(Ⅲ)/$MSiO_2$ **1** has not changed compare with the fresh catalyst (Fig. **S8** and Fig. **S9**)

Hence, we conclude that the leaching of Rh active centers is not the only reason for catalyst deactivation. In order to verify this conclusion, another experiment was carried out to restore the activity of the used catalyst. The recovered Rh(Ⅲ)/$MSiO_2$ **1** was dispersed in chlorobenzene, and then the system was heated to 60 ℃ for 8 h to remove the NBR glue on the surface or inside the pore of $MSiO_2$. In addition, the resulting catalyst was washed with acetone for three times and dried under vacuum at 60 ℃. After reactivation, the activity of Rh(Ⅲ)/$MSiO_2$ **1** was restored to 81.66% (Table **3**, cycle 4[a]), compare with 67.61% in the third recycle (Table **3**, cycle 3).

Therefore, the present results suggest a deactivation mechanism: a small quantity of Rh species (＜10 wt%) leach into the reaction solution, the SiO_2 particles re-aggregate, and the highly viscous NBR solution infiltrates the pores of the SiO_2, leading to a large mass transfer resistance.

Some fresh catalyst (15 wt% initial weight) was added along with the recovered catalyst from the first hydrogenation cycle to apply in hydrogenation of NBR, and the results are shown in Table **4**. With 15 wt% fresh catalyst added, the activity of the blend consisting of recovered and fresh catalyst was fully restored to 96.42%. After the three times cycle, the degree of hydrogenation for the blend still remains at 96.13%, an indication of the high stability and utility of the catalyst Rh(Ⅲ)/$MSiO_2$ **1**.

Table 4. Comparison of activity of fresh catalyst and blend of 15 wt% fresh catalyst and recovered catalyst

Recycle	1	2	3	4
HD (%)	97.53	96.42	95.88	96.13

Note: Reaction conditions: concentration of NBR solution=3 wt%, concentration of catalyst=5 wt%, $W_{PPh3}/W_{cat.}$= 0.5, P_{H2}=3.0 MPa, and T=120 ℃;

Further, this modification method is not restricted to the SiO_2 support and the Rh species. The hydrogenation of NBR was carried out by using other supports, such as the molecular sieves of 13X, MCM-41 and SBA-15. Fig. **S10** shows that before modification, the degree of hydrogenation of the

supported catalysts was 67.64%, 48.75%, and 67.42% for 13X, MCM-41, and SBA-15, respectively. After modification, the degree of hydrogenation for the supported catalysts increased to 96.34%, 89.46%, and 98.86%, respectively. These obvious increases show that modification of these supports with APTS enhances the activity of the Rh catalyst concerned. In addition, other congeneric transition metal (Ru^{3+} and Pd^{2+}) complexes deposited on the surface of modified SiO_2 also have enhanced catalytic performance (Fig. **S11**). For example, the degree of hydrogenation increases from 20.49% to 45.58% after modification for a Ru catalyst in hydrogenation of NBR. These results indicate that this method of surface modification by APTS can be extended to other catalyst systems to improve their activity, reusability, and stability.

4. Conclusions

The surface of SiO_2 was chemically modified with the silane coupling agent APTS, and Rh NPs are deposited on $MSiO_2$ surface to fabricate an Rh-loaded supported catalyst, Rh(Ⅲ)/$MSiO_2$. FTIR, SEM, XRD, XPS, BET, and ICP demonstrated that the Rh NPs were well dispersion on the surface of $MSiO_2$. In addition, the Rh(Ⅲ)/$MSiO_2$ showed a higher catalytic activity and stability in hydrogenation of NBR than Rh(Ⅲ)/SiO_2. Factors that influence the degree of hydrogenation were also fully investigated and the optimum reaction conditions were as follows: 200 mL of NBR solution (3 wt%), 0.12 g of supported catalyst (2 wt%), 0.06 g of triphenylphosphine (1 wt%), temperature of 140 ℃, H_2 pressure of 3.0 MPa, and reaction time of 8 h. A degree of hydrogenation above 98% was obtained. And the Rh(Ⅲ)/$MSiO_2$ could be recovered by a simple centrifugation and recycled for three consecutive runs with less loss of activity. After treatment of the recovered catalyst with chlorobenzene and acetone, the catalytic activity of the catalyst was restored from 67.61% to 81.66%. The enhanced interaction between the metal ions and the support, and the increase of the amount of metal species as well as their dispersion could be the reasons for the high activity of Rh(Ⅲ)/$MSiO_2$. This modified method may be a promising way to improve the activity and stability of other supported catalysts.

Acknowledgments

The financial supports of the National Natural Science Foundation of China under Grant No. 51221002 are gratefully acknowledged.

Notes and references

[a]State Key Laboratory of Organic-Inorganic Composites, Beijing University of Chemical Technology, Beijing 100029, China.
[b]Key Laboratory of Beijing City on Preparation and Processing of Novel Polymer Materials, Beijing 100029, China.
*Corresponding author: Dongmei Yue.
Tel: +86-010-64436201; Fax: +86-010-64436201.
E-mail address: yuedm@mail.buct.edu.cn.

1. K.-Y. Han, H.-R. Zuo, Z.-W. Zhu, G.-P. Cao, C. Lu and Y.-H. Wang, *Industrial & Engineering Chemistry Research*, 2013, **52**, 17750-17759.
2. S. Maheshwari, M. Tsapatsis and F. S. Bates, *Macromolecules*, 2007, **40**, 6638-6646.
3. H. Wang, Q. Pan and G. L. Rempel, *Journal of Polymer Science Part A: Polymer Chemistry*, 2012, **50**, 4656-4665.
4. H. Wang, Q. Pan and G. L. Rempel, *Journal of Polymer Science Part A: Polymer Chemistry*, 2012, **50**, 2098-2110.
5. L. Wei, J. Jiang, Y. Wang and Z. Jin, *Journal of Molecular Catalysis A: Chemical*, 2004, **221**, 47-50.
6. H. Wang, L. Yang and G. L. Rempel, *Polymer Reviews*, 2013, **53**, 192-239.
7. L. B. Dong, S. Turgman-Cohen, G. W. Roberts and D. J. Kiserow, *Industrial & Engineering Chemistry Research*, 2010, **49**, 11280-11286.
8. J. S. Parent, N. T. McManus and G. L. Rempel, *Industrial & Engineering Chemistry Research*, 1996, **35**, 4417-4423.
9. J. S. Parent, N. T. McManus and G. L. Rempel, *Industrial & Engineering Chemistry Research*, 1998, **37**, 4253-4261.
10. A. Mahittikul, P. Prasassarakich and G. L. Rempel, *Journal of Molecular Catalysis A: Chemical*, 2009, **297**, 135-141.
11. D. M. Yue, Z. M. Shen, R. Q. Xu and Y. K. Wei, *Journal of Elastomers and Plastics*, 2002, **34**, 225-237.
12. A. E. C. Collis and I. T. Horvath, *Catalysis Science & Technology*, 2011, **1**, 912-919.
13. J. M. Thomas, J. C. Hernandez-Garrido, R. Raja and R. G. Bell, *Physical Chemistry Chemical Physics*, 2009, **11**, 2799-2825.
14. Y. Kubo and K. Ohura, US Patents, 1982.
15. Y. Kubo and K. Oura, US Patents, 1984.
16. H. Dai, H. Li and F. Wang, *Applied Surface Science*, 2006, **253**, 2474-2480.
17. G. O. Williams, G. M. O'Connor, P. T. Mannion and T. J. Glynn, *Applied Surface Science*, 2008, **254**, 5921-5926.
18. R. Chen, Y. Jiang, W. Xing and W. Jin, *Industrial & Engineering Chemistry research*, 2011, **50**, 4405-4411.
19. H. Wu, Z. Liu, X. Wang, B. Zhao, J. Zhang and C. Li, *Journal of Colloid and Interface Science*, 2006, **302**, 142-148.
20. S. J. J. Titinchi and H. S. Abbo, *Catalysis Today*, 2013, **204**, 114-124.
21. I. Slowing, B. G. Trewyn and V. S. Y. Lin, *Journal of the American Chemical Society*, 2006, **128**, 14792-14793.

22. V. Antochshuk, O. Olkhovyk, M. Jaroniec, I.-S. Park and R. Ryoo, *Langmuir*, 2003, **19**, 3031-3034.
23. F. Balas, M. Manzano, P. Horcajada and M. Vallet-Reg í, *Journal of the American Chemical Society*, 2006, **128**, 8116-8117.
24. A. M. Liu, K. Hidajat, S. Kawi and D. Y. Zhao, *Chemical Communications*, 2000, 1145-1146.
25. X. Wang, K. S. K. Lin, J. C. C. Chan and S. Cheng, *The Journal of Physical Chemistry B*, 2005, **109**, 1763-1769.
26. D. J. Macquarrie and D. B. Jackson, *Chemical Communications*, 1997, 1781-1782.
27. H. Li, H. Jiang, R. Chen, Y. Wang and W. Xing, *Industrial & Engineering Chemistry Research*, 2013, **52**, 14099-14106.
28. A. J. Marshall, I. R. Jobe, T. Dee and C. Taylor, *Rubber Chem. Technol.*, 1990, **63**, 244-255.
29. C.-H. Huang, K.-P. Chang, H.-D. Ou, Y.-C. Chiang and C.-F. Wang, *Microporous and Mesoporous Materials*, 2011, **141**, 102-109.
30. L. Yan, Y. J. Ding, H. J. Zhu, J. M. Xiong, T. Wang, Z. D. Pan and L. W. Lin, *Journal of Molecular Catalysis A: Chemical*, 2005, **234**, 1-7.
31. I. Lee, M. A. Albiter, Q. Zhang, J. Ge, Y. Yin and F. Zaera, *Physical Chemistry Chemical Physics*, 2011, **13**, 2449-2456.
32. F. Zaera, *Chemical Society Reviews*, 2013, **42**, 2746-2762.
33. W. Long, N. A. Brunelli, S. A. Didas, E. W. Ping and C. W. Jones, *Acs Catalysis*, 2013, **3**, 1700-1708.
34. S. Moussa, A. R. Siamaki, B. F. Gupton and M. S. El-Shall, *Acs Catalysis*, 2012, **2**, 145-154.